Antivortex state in crosslike nanomagnets

V. L. Mironov,* O. L. Ermolaeva, S. A. Gusev, A. Yu. Klimov, V. V. Rogov, B. A. Gribkov, O. G. Udalov, and A. A. Fraerman
Institute for Physics of Microstructures, RAS, Nizhny Novgorod 603950, GSP-105, Russia

R. Marsh, C. Checkley, R. Shaikhaidarov, and V. T. Petrashov
Department of Physics, Royal Holloway, University of London, Egham, Surrey TW20 0EX, United Kingdom
(Received 5 November 2009; revised manuscript received 2 February 2010; published 30 March 2010)

We report on results of computer micromodelling of antivortex states in asymmetrical crosslike ferromagnetic nanoparticles and their practical realization. The arrays of cobalt crosses with 1 μm branches, 100 nm widths of the branches and 40 nm thicknesses, were fabricated using e-beam lithography and ion etching. Each branch of the cross was tapered at one end and bulbous at the other. The stable formation of antivortex magnetic states in these nanostructures during magnetization reversal was demonstrated experimentally using magnetic force microscopy.

DOI: 10.1103/PhysRevB.81.094436 PACS number(s): 75.75.−c, 07.79.Pk, 75.60.Ch, 75.40.Mg

I. INTRODUCTION

Technological applications as well as fundamental investigations of magnetic nanostructures, the so-called nanomagnets, require well-controlled magnetic states. Examples are the single-domain nanomagnets that are very promising candidates for high-density hard disk data storage and integrated magnetoelectronic devices such as nonvolatile magnetic memory,[1] nanomagnets with noncollinear magnetization, which show a novel type of "helical" triplet superconductivity,[2] and noncoplanar nanomagnets for which novel transport properties are expected.[3–5] One of the controls of the magnetic states at the nanometer scale is the size and geometry of nanoelements. Very small nanomagnets at the 10 nm scale are expected to behave as single giant spins, since competition between magnetostatic energy and quantum-mechanical exchange energy entirely suppresses magnetic domain formation. A range of interesting phenomena takes place in the intermediate ("mesoscopic") range of 10–1000 nm, where electron-beam lithography allows for "magnetic nanoengineering" with well-defined geometry of nanostructures. Highlights are the realization of vortex states in ferromagnetic nanodisks,[1] spiral (helical) states in laterally confined magnetic multilayers,[6] and the prediction of a novel type of magnetic wall in nanoconstrictions.[7]

In this paper we report on theoretical and experimental studies of another fundamental magnetization structure, the antivortex,[8–10] which is a topological counterpart of a magnetic vortex. Besides being a remarkable magnetic structure, the antivortex is expected to show unusual transport properties in an applied external magnetic field, namely, a spectacular new phenomenon, the so-called "topological" Hall effect.[11]

Unlike a vortex, the realization of an antivortex, i.e., the preparation of a nanostructure that contains only a single antivortex, is a challenging task. The antivortex possesses a "magnetic charge" resulting in additional magnetostatic energy, in comparison with a vortex.

We start with consideration of the distribution of magnetization in sufficiently thin ferromagnetic disks. In this case the magnetization depends only on the in-plane coordinates $\vec{M}(\vec{\rho})$, where $\vec{\rho}$ is the in-plane radius vector. In the absence of magnetocrystalline anisotropy and an external magnetic field the symmetric inhomogeneous distribution of magnetization in a circular disk can be represented in the following generalized form:[12]

$$M_x = \sin\,\theta(\rho)\cos(\nu\varphi + \varphi_0),$$

$$M_y = \sin\,\theta(\rho)\sin(\nu\varphi + \varphi_0),$$

$$M_z = \cos\,\theta(\rho), \tag{1}$$

where ρ is the modulus of the radius vector $\vec{\rho}$, θ and φ are polar and azimuth angles, respectively, φ_0 is an arbitrary phase shift, and $\nu = 0, \pm 1, \pm 2, \ldots$ is the so-called "winding number." The topology of the magnetic state [Eq. (1)] is determined by the phase shift φ_0, direction of core magnetization [$\cos\,\theta(\rho=0)=p$] and winding number ν. For a disk of sufficiently small radius and thickness, the ground state is the uniform single-domain state ($p=\nu=0$). In general, nonuniform distributions can be realized with a magnetic structure determined by these parameters with polar angle independent of the phase shift φ_0 and the sign of the winding number. For $\nu=1$, $\varphi_0=\pm\pi/2$, we have the well-known vortex states, where the sign of the phase shift φ_0 corresponds to clockwise and counter clockwise vortices [Fig. 1(a)]. For $\nu=1$, $\varphi_0=0,\pi$, we have a hedgehoglike distribution [Fig. 1(b)]. The set of parameters $\nu=-1$, $\varphi_0=0,\pi$ corresponds to the antivortex states [Fig. 1(c)]. The antivortex and hedgehoglike states are not realized in circular nanodisks spontaneously, since they are accompanied by the formation of effective magnetic charges on the side walls that considerably increase the magnetostatic energy of this system in comparison with the vortex state. Besides, in contrast to the vortex state, the antivortex magnetization distribution has volume magnetic charges with the density

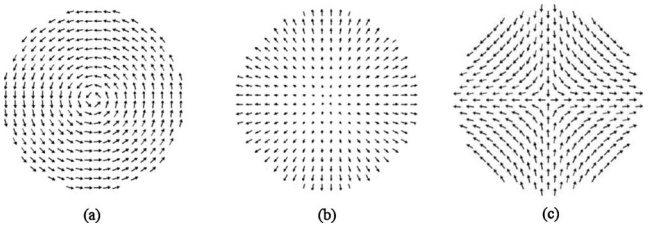

FIG. 1. The distributions of magnetization for the magnetic states with winding number equal to one. (a) is a vortex state $\nu=1$, $\varphi_0=+\pi/2$, (b) is a hedgehoglike state $\nu=1$, $\varphi_0=0$, and (c) is an antivortex state $\nu=-1$, $\varphi_0=0$.

$$div\ \vec{M} \sim \pm \frac{1}{\rho}\cos 2\varphi, \quad \rho \gg l, \tag{2}$$

where the sign $\pm$ corresponds to the phase shift $\varphi_0=\pi,0$, l is the antivortex core radius, which is typically about 20 nm for transition metals. This volume magnetic charge produces a magnetic stray field and as a result we have an additional contribution to the energy of the antivortex, which is proportional to the particle volume. Nevertheless the hedgehoglike and antivortex states can be stabilized by external factors. For example, the hedgehoglike state can be realized in a circular nanodisk under the influence of inhomogeneous external magnetic field induced by a magnetic force microscope (MFM) tip.[13]

The antivortex distribution can be stabilized by the transformation of the shape of the magnetic particle from circular to crosslike. This shape variation leads to the quasivortex state formation in the crosses with relatively small aspect ratio $g=a/b$ $(g>1)$ [Fig. 2(a)]. An increase in the aspect ratio leads to an increase in the magnetostatic energy and results in the stabilization of quasiuniform [Fig. 2(b)] and antivortex [Fig. 2(c)] states. However due to the volume charge, the energy of the antivortex distribution in crosslike structures is larger than the energy of a quasiuniform distribution, making realization of the antivortex state a hard problem.

A few years ago, an antivortex structure was created in a cross junction of four connected rings[10] with vortex distribution in each of the rings. This was a complicated design that did not allow for transport measurements, especially in an external magnetic field. In this work a single-antivortex state has been realized in asymmetric crosslike nanomagnets suitable for Hall effect measurements. The antivortex state is prepared by means of a specific procedure of magnetization reversal stimulated by the shape asymmetry.

As has been mentioned above, one of the reasons for interest in such "exotic" nonuniform and noncoplanar magnetic structures as antivortices is due to their unusual electron-transport properties, in particular, the topological Hall effect (THE). The winding number ν defined in formula (1) has a direct impact on the electron transport.[14,15] This can be seen from the following formulas for the contribution of THE to the Hall current:[5]

$$\vec{j}_{\mathrm{THE}} = [\vec{E} \times \vec{B}^{eff}],$$

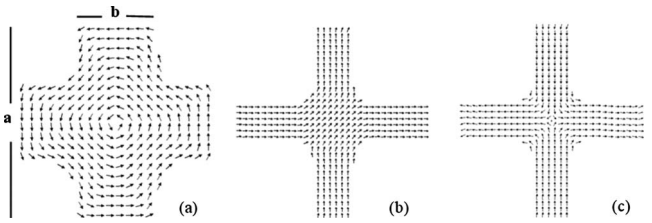

FIG. 2. The model distributions of magnetization in crosslike elements. (a) is for quasivortex state, (b) is for quasiuniform state, and (c) is for antivortex state.

$$B_x^{eff} = \alpha\left(\vec{m} \cdot \left[\frac{\partial \vec{m}}{\partial y} \times \frac{\partial \vec{m}}{\partial z}\right]\right),$$

$$B_y^{eff} = \alpha\left(\vec{m} \cdot \left[\frac{\partial \vec{m}}{\partial z} \times \frac{\partial \vec{m}}{\partial x}\right]\right),$$

$$B_z^{eff} = \alpha\left(\vec{m} \cdot \left[\frac{\partial \vec{m}}{\partial x} \times \frac{\partial \vec{m}}{\partial y}\right]\right), \tag{3}$$

where the $\vec{B}^{eff}$ is the effective additional magnetic field acting on the conduction electrons in the medium with nonuniform and noncoplanar magnetization; the constant α is on the order of the flux quantum $\Phi_0 \sim 10^{-7}$ Oe cm^2;[4,15] $\vec{m}$ is the unit vector parallel to the local magnetization. Using Eqs. (1) and (3) one obtains the following expression for the effective magnetic field B^{eff} in the case of vortex and antivortex

$$B_z^{eff}(\rho) \sim \alpha\nu\frac{1}{\rho}\frac{\partial m_z}{\partial \rho}; \quad B_x^{eff} = B_y^{eff} = 0. \tag{4}$$

It is seen from Eq. (4) that the sign of the topological Hall current is determined by the winding number and by the core polarization (p) and does not depend on the phase shift φ_0. The topological Hall effect has opposite signs for the vortex and antivortex structures of the same core polarization.

The aim of this work is the realization of the antivortex state in magnetic nanostructures, which is an interesting and nontrivial problem in itself, in a geometry which allows for an investigation of its extraordinary electron-transport properties.

This paper has the following structure. In Sec. II we present the results of computer micromagnetic modeling of the magnetization reversal process in an asymmetrical cross. Section III is devoted to the description of experimental results, which illustrate the practical realization of antivortex states in asymmetrical cobalt crosses.

II. COMPUTER MICROMAGNETIC MODELING

The micromagnetic modeling of magnetic states was based on the numerical solution of the Landau-Lifshitz-Gilbert (LLG) equation[16] for the magnetization $\vec{M}(\vec{r},t)$

$$\frac{\partial \vec{M}}{\partial t} = -\gamma(\vec{M} \times \vec{H}_{eff}) - \frac{\gamma d}{M_s}[\vec{M} \times (\vec{M} \times \vec{H}_{eff})], \tag{5}$$

where γ is the gyromagnetic ratio, d is the dimensionless damping parameter, and M_s is the magnetization at satura-

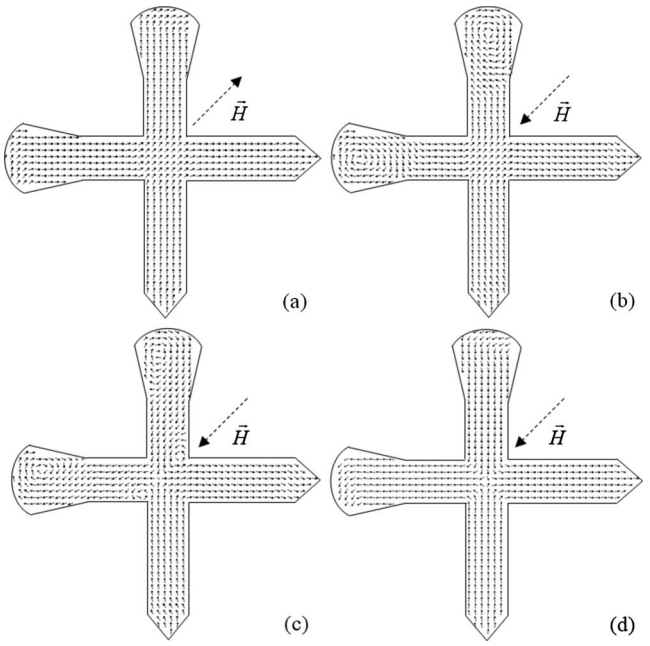

FIG. 3. The formation of an antivortex state during the remagnetization of an asymmetrical cross in an external magnetic field. (a) is the initial distribution of magnetization, (b) is the nucleation of vortices in the reversed external magnetic field, (c) is the nucleation of an antivortex core and formation of additional vortices, and (d) is the final antivortex state. The lateral size of the crosses a was about 1 μm; the width of the segments b was 100 nm and size of the bulb was 150 nm.

tion. The effective field $\vec{H}_{eff}=-\frac{\delta E}{\delta \vec{M}}$ is a variation derivative of the energy function. The total energy of the particle can be defined by

$$E = E_{ex} + E_m + E_a + E_h. \tag{6}$$

The first term E_{ex} is the energy of the exchange interaction, the second term E_m is the demagnetization energy of the disk, and E_a is the magnetic crystalline anisotropy energy. Expressions for these terms have conventional form (see, for example, Ref. 17). The last term E_h is the energy of the interaction between the particle magnetization and an external magnetic field $\vec{H}$.

The calculations were performed using standard (object oriented micromagnetic framework) software.[18] All calculations were carried out for parameters of cobalt $J=10^{-6}$ erg/cm, $M_s=1400$ emu/cm^3, and damping constant $d=0.5$. We omitted the magnetic anisotropy term in Eq. (6), assuming polycrystalline structure of the particles. The form of cross-shaped particles was defined by special graphic masks created in standard graphic software (windows paint, for example). The model distributions were obtained as the stationary solutions of the system of LLG equations for the magnetization on a square grating. The grating cell size has been selected to be near 5 nm.

In the model calculations we have taken into account the dependence of the coercivity of magnetic elements on their shape[19] and considered an asymmetrical cross shown in Fig. 3. The magnetic structure in the cross can be manipulated by an external magnetic field directed along the nonsymmetrical diagonal of the cross as follows. (a) After magnetizing in a sufficiently strong ($\sim$1 kOe) magnetic field applied along the nonsymmetrical diagonal, we obtained a quasiuniform distribution [Fig. 3(a)]. (b) Then, under the action of a certain magnetic field H with magnitude $H_1<H<H_2$ (H_1 and H_2 are the coercivity of bulbous and tapered ends, respectively) oriented in the opposite direction, we observed at the first stage the nucleation of vortices in the bulbous segments [Fig. 3(b)]. (c) At the second stage, the nucleation of an antivortex core with extra two vortices near the center of the cross [Fig. 3(c)] was observed. (d) At the final stage, the annihilation of the vortices and the formation of the antivortex distribution of magnetization in the cross were observed [Fig. 3(d)].

The magnetization in the tapered elements was kept in the initial uniform state at all stages. Thus after the action of the reversed magnetic field $H_1<H<H_2$ we obtained the antivortex distribution.

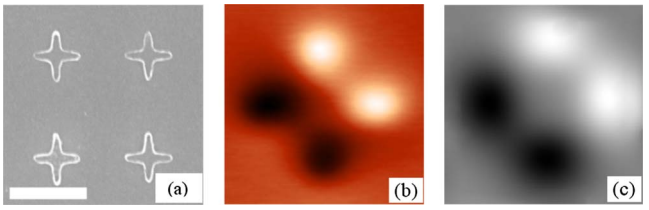

FIG. 4. (Color online) (a) is SEM image of an array of symmetric crosslike cobalt nanostructures. The scale bar is 1 μm. The normalized experimental (b) and model (c) MFM contrast distributions corresponding to the A type of quasiuniform state [Fig. 2(b)] of magnetization (arbitrary units).

III. EXPERIMENTAL RESULTS

The arrays of Co crosses were fabricated using a negative e-beam lithography process. A film of Co with thickness 40 nm was deposited onto a Si substrate using magnetron sputtering and covered with 100 nm thick positive UV photoresist (FP-9120), which is based on phenol-aldehyde resin. The protective masks were formed in the photoresist by exposure in the ELPHY PLUS system based on the scanning electron microscope SUPRA 50VP with subsequent chemical treatment in an organic solvent. At the final stage, the nanoarrays were fabricated by Ar^+-ion etching.

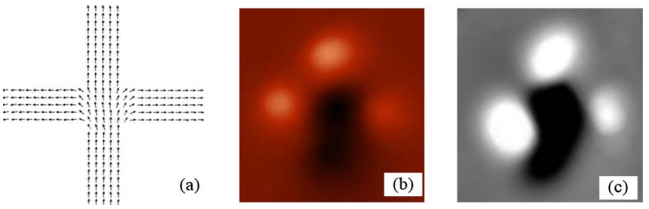

FIG. 5. (Color online) (a) is the B-type quasiuniform state with three incoming and one outgoing magnetization vectors (simulation). The normalized experimental (b) and model (c) MFM contrast distribution corresponding to the B type of quasiuniform state of magnetization (arbitrary units).

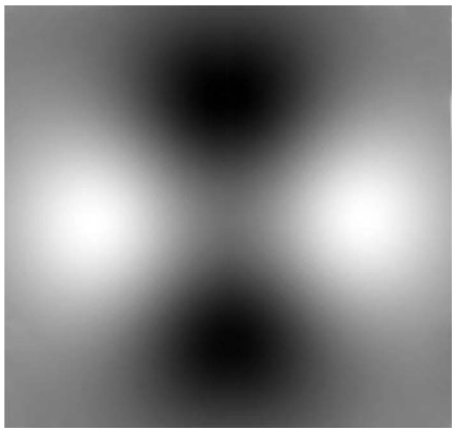

FIG. 6. The model MFM contrast distribution corresponding to the antivortex state [Fig. 2(c)] of magnetization (arbitrary units).

The magnetic states in the Co crosses and the magnetization-reversal effects were studied *in situ* using a vacuum multimode scanning probe microscope "Solver-HV," which was equipped with a dc electromagnet incorporated in a vacuum vibration insulating platform. The scanning probes were cobalt coated with a thickness of 30 nm. Before measurements, the tips were magnetized along the symmetry axes (Z) in a 10 kOe external magnetic field. The MFM measurements were performed in the noncontact constant height mode. The phase shift, $\Delta\varphi$, of cantilever oscillations under the gradient of the sample magnetic field was registered to obtain the MFM contrast. The model MFM contrast was calculated in the linear point-mass approximation[20,21]

$$\Delta\varphi = -\frac{Q}{K}\frac{\partial F_z}{\partial z}, \tag{7}$$

where Q is the cantilever quality factor, K is the cantilever force constant, and F_z is the z component of the force caused by sample stray magnetic field. For the simplest tip model, the value $\Delta\varphi$ is proportional to the second derivative of the z component of magnetic stray field $\partial^2 H_z/\partial z^2$. The model MFM images were calculated on the basis of model magnetization distributions in the dipole-dipole approximation.

All measurements were performed in a vacuum of 10^{-4} Torr, which improved the MFM signal due to an increase in the cantilever quality factor. The first set of measured samples consisted of symmetric crosses. Their magnetic structure depended on the aspect ratio, as expected. The crosses with relatively large aspect ratio g showed spontaneous quasiuniform states. Spontaneous quasiuniform states were observed in the crosses with lateral size $a=600$ nm and width of branch $b=100$ nm: ($g=6$). The states showed two types of symmetries: (i) state A [with two incoming and two outgoing magnetization vectors, see Fig. 2(b)] and (ii) state B with three incoming (outgoing) and one outgoing (incoming) magnetization vectors [see Fig. 5(a)]. Experimental MFM images of these states are shown in Figs. 4(b) and 5(b). Figures 4(c) and 5(c) show the corresponding model MFM contrast distributions. A characteristic feature of A and B quasiuniform states is the four-pole symmetry of the MFM contrast distribution. The bright poles on the MFM pictures correspond to the magnetic poles of sample magnetization coinciding with the tip magnetic pole; and the dark poles correspond to the reciprocal magnetic poles. With this taken into account, the MFM contrast of the antivortex distribution [Fig. 2(c)] is expected to have specific symmetry with like

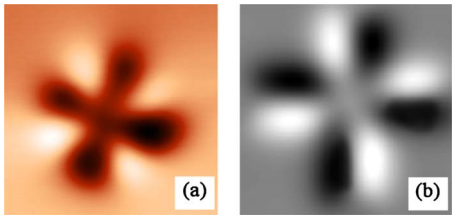

FIG. 7. (Color online) The normalized experimental (a) and model (b) MFM contrast distributions corresponding to the quasivortex distribution [Fig. 2(a)] of magnetization (arbitrary units).

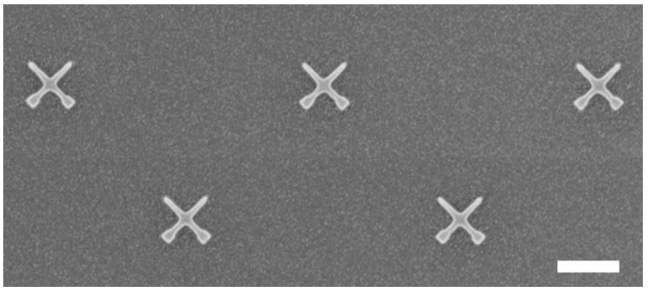

FIG. 8. SEM image of asymmetric Co nanocrosses. The white scale bar is 1 μm.

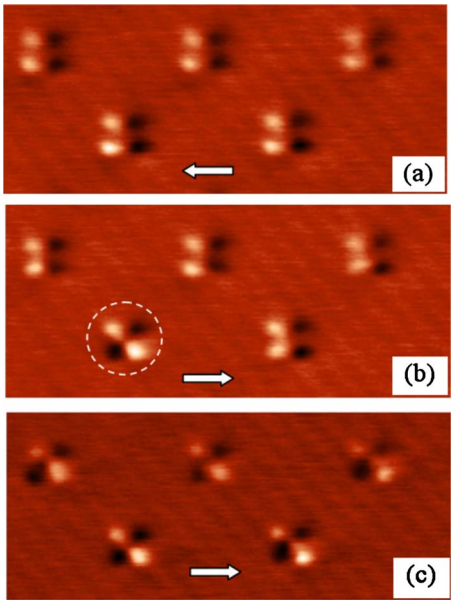

FIG. 9. (Color online) Transformation of magnetic states in asymmetric Co crosses from quasiuniform states to antivortex states in an external magnetic field. (a) is MFM image of the initial quasiuniform state. (b) is MFM image of the same array of crosses in a weak (250 Oe) reversed magnetic field. The cross with antivortex state is indicated by a white circle. (c) is MFM image of the final antivortex states. The directions of the applied magnetic fields are indicated by white arrows. The frame size is 6×12 μm^2.

poles situated in the opposite positions. This is confirmed by the model MFM image for the antivortex distribution shown in Fig. 6.

For the crosses with relatively small aspect ratio (lateral size $a=600$ nm and width of branch $b=200$ nm; $g=3$) the quasivortex states were registered. The experimental MFM image of the quasivortex state and the corresponding model picture are presented in Fig. 7. The symmetry of MFM contrast has a fourfold axis corresponding to the quasivortex magnetization distribution [Fig. 2(a)].

To realize the antivortex state, we fabricated asymmetrical crosses similar to those used in micromagnetic modeling (see Fig. 3). An SEM image of the fabricated structure is shown in Fig. 8. The lateral size of the crosses was $a=1$ μm, the width of the branch was $b=100$ nm ($g=10$) and the size of bulbs was 150 nm. Figure 9 shows the results of the *in situ* remagnetization experiments with such asymmetric crosses. The remagnetization was done in several stages.

(a) At the first stage, a strong (800 Oe) magnetic field was applied along the nonsymmetrical diagonal of the cross [as shown in Fig. 3(a)]. It formed a quasiuniform magnetization [Fig. 9(a)].

(b) Second, a weak reversed magnetic field with magnitude of 250 Oe was applied. This led to the transition of one of the particles into an antivortex state with characteristic four-pole symmetry. The cross with antivortex state is indicated in Fig. 9(b) by the circle.

(c) Further increase in the external magnetic field leads to the transition to antivortex states of the rest of the crosses [Fig. 9(c)]. The observed dispersion of switching fields from 250 to 400 Oe for this set of crosses can be attributed to the dispersion in the coercive forces due to the shape variations.

IV. CONCLUSIONS

We have reported the results of micromagnetic modeling and experimental investigations of magnetic states in ferromagnetic crosslike nanomagnets. It was shown that the shape control based on electron-beam lithography allows for practical "nanoengineering" of magnetic states in crosslike nanostructures. We have demonstrated that symmetric Co nanocrosses can be put into spontaneous quasiuniform and quasivortex states depending on their size and their aspect ratio. The asymmetrical Co crosses, where each branch is tapered at one end and bulbous at the other, showed the stable formation of antivortex states during magnetization reversal in an external magnetic field. These structures with well-controlled quasiuniform and antivortex states are very promising for investigations of transport peculiarities and magnetodynamical phenomena specific to inhomogeneous magnetic systems.

ACKNOWLEDGMENTS

This work was supported by the Russian Foundation for Basic Research (Project No. 08-02-01202), Russian Federal Educational Agency (Contracts No. P 348 and No. P 417), Russian Federation President's grant for support of young scientists (Grant No. MK-4508.2009.2), and the U.K. EPSRC (Grant No. EP/F016891/1). We send our special thanks to the reviewers for the very useful comments.

*mironov@ipm.sci-nnov.ru

[1] R. P. Cowburn, D. K. Koltsov, A. O. Adeyeye, M. E. Welland, and D. M. Tricker, Phys. Rev. Lett. **83**, 1042 (1999).
[2] I. Sosnin, H. Cho, V. T. Petrashov, and A. F. Volkov, Phys. Rev. Lett. **96**, 157002 (2006).
[3] A. A. Fraerman and O. G. Udalov, Phys. Rev. B **77**, 094401 (2008).
[4] P. Bruno, V. K. Dugaev, and M. Taillefumier, Phys. Rev. Lett. **93**, 096806 (2004).
[5] O. G. Udalov and A. A. Fraerman, arXiv:0907.1808 (unpublished).
[6] A. A. Fraerman, B. A. Gribkov, S. A. Gusev, A. Yu. Klimov, V. L. Mironov, D. S. Nikitushkin, V. V. Rogov, S. N. Vdovichev, B. Hjorvarsson, and H. Zabel, J. Appl. Phys. **103**, 073916 (2008).
[7] P. Bruno, Phys. Rev. Lett. **83**, 2425 (1999).
[8] S. Gliga, M. Yan, R. Hertel, and C. M. Schneider, Phys. Rev. B **77**, 060404(R) (2008).
[9] H. Wang and C. E. Campbell, Phys. Rev. B **76**, 220407(R) (2007).
[10] K. Shigeto, T. Okuno, K. Mibu, T. Shinjo, and T. Ono, Appl. Phys. Lett. **80**, 4190 (2002).
[11] A. Neubauer, C. Pfleiderer, B. Binz, A. Rosch, R. Ritz, P. G. Niklowitz, and P. Böni, Phys. Rev. Lett. **102**, 186602 (2009).
[12] A. M. Kosevich, V. P. Voronov, and I. V. Manzhos, Sov. Phys. JETP **57**, 86 (1983).
[13] V. L. Mironov and A. A. Fraerman, in *Electromagnetic, Magnetostatic, and Exchange-Interaction Vortices in Confined Magnetic Structures*, edited by E. O. Kamenetskii (Research Signpost, Kerala, India, 2008), pp. 159–175.
[14] A. A. Thiele, Phys. Rev. Lett. **30**, 230 (1973).
[15] Ya. Aharonov and A. Stern, Phys. Rev. Lett. **69**, 3593 (1992).
[16] W. F. Brown, *Micromagnetics* (Wiley, New York, 1963).
[17] E. D. Boerner and H. N. Bertran, IEEE Trans. Magn. **33**, 3052 (1997).
[18] http://math.nist.gov/oommf
[19] J.-G. Zhu, Y. Zheng, and G. A. Prinz, J. Appl. Phys. **87**, 6668 (2000).
[20] D. Rugar, H. J. Mamin, P. Guethner, S. E. Lambert, J. E. Stern, I. McFadyen, and T. Yogi, J. Appl. Phys. **68**, 1169 (1990).
[21] R. D. Gomez, E. R. Burke, and I. D. Mayergoyz, J. Appl. Phys. **79**, 6441 (1996).